COMARISON OF TWO DIFFERENT INDICATORS FOR HOT CRACKING IN WELDED STRUCTURES

J Edberg*, J Draxler*, J Andersson**
***Luleå University of Technology, ****University West**

Keywords: *hot cracking, welding, indicator*

Abstract

Welding simulations of the nickel-based superalloy Alloy 718 have been performed, combined with two fundamentally different hot crack indicators. The purpose of the indicators was to evaluate the risk of hot crack development in the weld. The result of the simulations has been compared with experiments. Advantages and limitations of the two hot crack indicators are discussed. Regions with a high value of the indicators in the simulations agree well with regions with hot cracks in the experiments.

1 Introduction

Fuel consumption and environmental impact have become an important issue for the aerospace industry, and it will be even more important in the future. In order to provide a more environmentally friendly production and operation of the equipment, the weight of the structure has to be reduced. This will affect the fuel consumption during operation, but also make more efficient use of resources during manufacturing. Weight reduction requires higher strength of the materials in use. Therefore, it is desirable to replace cast material with hot and cold worked material with better mechanical properties. Here welding plays an important role since hot and cold worked sub-components have to be joined together in order to produce more complicated parts. Many parts in a jet engine are made from nickel-based superalloys in order to withstand the high operating temperatures. However, weld hot cracking of Ni-based superalloys is a serious problem, both in manufacturing and overhaul since it endangers component life if cracks are allowed to propagate.

Simulation of the manufacturing process, including welding, is an important tool when optimizing the manufacturing process in order to improve the quality of the product. The finite element method (FEM) is widely used for this purpose. Using FEM, it is possible to simulate the effect of different welding patterns, for example. It is desirable that, in these simulations, an index of the risk of cracks could be presented in an easy way. But FE-based crack criteria that can predict the risk of cracking due to welding or heat treatments are rare. There are also many different types of cracks that can appear in a weld and in its surroundings. In this paper, we focus on weld hot cracks. These are cracks that form during the solidification of the weld.

Two different hot crack indexes are compared with Varestraint tests. One is a relatively simple, based on the assumption that cracks will form if the material is subjected to strains above a critical limit within a sensitive temperature interval. This is called the intuitive crack criteria in the text below. The other hot crack index is more advanced and has a much deeper theoretical background. Hot cracks are assumed to form by rupture of grain boundary liquid films, due to localization of strain during the solidification. This is called the physically based crack criteria in the text below.

Further descriptions of both hot crack indexes can be found below.

Fig. 2. Varestraint test equipment.

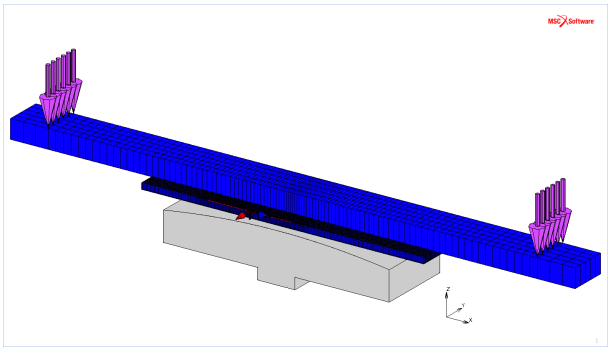

Fig. 1. Finite element mesh.

2 Experiment

The Varestraint test equipment at GKN Aerospace Engine Systems in Sweden was used in the experiment [1]. The machine, shown in Figure 1, was designed to meet a range of requirements and consists of three units that are synchronized with each other: a hydraulic part, a 100 ton capability press, and a welding robot.

The test parameters are: radius of the die block (150, 200, 300, 400 and 500 mm), the welding speed (1.0 mm/s), stroke rate (10 mm/s), and weld current (80 A). Test sample geometry (150x60x3.2 mm), material of testing (Alloy 718 sheet, continuous mill annealed condition) and welding process (gas tungsten arc welding), were kept constant during all the tests, as well as the placement of test samples in the equipment.

Two expendable SS304 support bars were used on top of the test samples to make sure the test samples conformed to the specific radius in an ideal way without hinging. The welding takes place between the support bars.

3 Theoretical analysis

The mechanical and thermal analysis is performed by the finite element method. The approach is the same as in classical Computational Welding Mechanics (CWM) [2].

3.1 Finite element program

The finite element program MSC Marc was used in this study [3]. This is a non-linear finite elements analysis software that can be used to simulate complex materials behavior and interaction under large deformations and strains. It can also be used for various multi-physics problems, in this case a thermal-mechanical coupled problem. It also supports automatic two-dimensional and three-dimensional re-meshing to analyze structures that undergoes large deformations, a feature that was used in this work. Not because the deformations are large, but because the welding process creates sharp temperature and strain gradients in the welded material.

3.2 Finite element model

Similar finite element meshes where used for simulations using any of the two hot crack criteria. The difference is that automatic re-meshing is enabled for simulations with the physically based crack criteria. This feature is disabled for simulations using the intuitive crack criteria. The finite element mesh can be seen in Figure 2. It initially consists of 39900 elements and 48675 nodes. This increase when automatic re-meshing is performed. Due to symmetry only one half of the plate and one of the support bars are analyzed.

The simulation starts with 40 seconds of welding until the heat source of the weld is positioned directly above the center of the die block. Then the hydraulic press moves down with 10 mm/s and the welding continues for another 5 seconds. Then the plate is allowed to cool down.

The material of the die block and the hydraulic press is assumed to be rigid. The data for Alloy 718 and SS304 were obtained from the suppliers of these materials. The center of the test plate is in direct contact with the die at the start

of the simulation and also in direct contact with the support bars. The support bars are also in direct contact with the hydraulic press at the start of the simulation.

Quasi-static mechanical condition was assumed, and transient temperature evolution. The yield condition according to von Mises and the associated flow rule were used. The hardening was assumed to be isotropic.

4 Hot crack criteria

Two hot crack criteria were investigated. The first criterion is based on intuition and common knowledge about solidification of alloys. The second criteria have a physical background.

4.1 Intuitive hot crack criteria

The intuitive hot crack criterion is based on the following assumptions:

- The material cannot carry any tensile stress above the coherent temperature.
- Cracks cannot form at temperatures above the coherent temperature.
- The material cannot carry any real load above the solidus temperature.
- Cracks form above the solidus temperature.
- Cracks only form when the temperature is decreasing.

A detailed description of this hot crack indicator can be found in [4].

Hot cracks will form if the material is deformed above a critical limit, within a critical temperature interval. The boundaries for this temperature interval are (in theory) the coherent temperature and the solidus temperature. In practice these temperatures are evaluated from crack investigations performed after a Varestraint test.

Hot cracks appear when the plastic deformation, within the sensitive temperature range reach a critical value. The hot crack indicator is scaled accordingly so that it reaches a value of 1.0 when the critical plastic strain within the sensitive temperature range is reached. Temperatures, stresses, and strains were calculated using FEM. One of the assumptions is that the material cannot carry any real load above the solidus temperature. But stress is not a part of the criteria. Instead, we only tolerate a small amount of plastic deformation when the material is in the critical temperature range between the solidus temperature and the coherent temperature, regardless of stress. When that plastic deformation reaches a critical value, the crack indicator reaches the value 1.0. This value can be plotted at a specific time for the whole finite element model, or as a function of time for a selected point in the finite element model after a successful simulation. The crack criterion has been implemented as a user subroutine in MSC Marc. All needed parameters for this criterion come from the CWM simulation or from parameters evaluated from the Varestraint test.

4.2 Physically based hot crack criteria

When this crack criterion is used, the result from CWM simulations are post-processed and combined with detailed models of the metallurgy as well as the behavior of the liquid film between grain boundaries (GBLF). All in order to estimate the risk for hot crack initiation. The theory behind this crack index can be divided in two parts. The first part describes a model for pore growth in the liquid film between two grains. It is assumed that rupture initiates when the grain boundary liquid pressure reaches a critical value. Then a pore can grow into a crack. This is a phenomenon that has been observed in in situ experiments [5]. The critical pressure is the pressure required to overcome the capillarity forces at the liquid-gas interface of the pore. Thus, the liquid pressure is believed to be of major importance for hot crack nucleation. The pore will shrink or grow depending on the pressure, or rather under-pressure, in the liquid film. If it does not shrink before solidification, it becomes a crack initiation site. The model for pressure in the liquid film is a central component in this crack criterion.

It is not fully understood how hot cracks form. The book by Campbell [6] describes various nucleation theories of hot cracks. Even so, we assume that there are pores in the material, but the mechanisms for the actual creation of the pores are not considered. The model describes

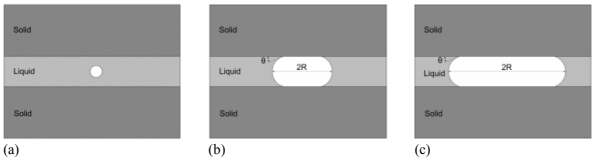

Fig. 3. Schematic representation of a pore growing from a sphere into a disc.

how an existing pore grows or shrinks. The shape is assumed to depend on the size of the pore compared to the thickness of the GBLF. At some instance, after the nucleation, the pore is assumed to grow with a spherical shape as shown in Figure 3(a). It is assumed to grow until the radius is the same as the half GBLF thickness. After that, it is assumed to grow as a disc, see Figure 3(b) and 3(c). The shape of the pore profile depends on interfacial energies, the pressure difference across its boundary, and the thickness of the GBLF. The difference between the pressure inside the pore and the external surrounding liquid pressure outside the pore was calculated by Young-Laplace equation. The assumptions that the gas inside the pore is an ideal gas, and that no gas is diffusing to the pore during the solidification were used. A detailed description of the theory can be found in [7].

A hot crack initiation index (HCII) was defined as the ratio between the liquid pressure drop and the liquid pressure drop for an infinite large pore. For a growing disc pore with a large radius, the surrounding liquid pressure approaches the critical pressure for pore growth, described above. We assumed that a HCII value larger than 1.0 lead to crack initiation. The liquid flow is assumed to be confined into a single GBLF where the liquid pressure was computed from a combination of Reynold's equation and Darcy's equation depending on the amount of solidified material [8]. The GBLF was assumed to be located between columnar grains that have grown parallel to the liquidus isotherm with zero undercooling to solidification. The solidification of the liquid phase was governed by a multicomponent Scheil model. During the solidification, all mechanical strains are assumed to be concentrated in the grain boundary liquid films.

In order to account for strain localization in the GBLF, a temperature dependent length scale was used. The length scale corresponds to a local region around the GBLF where all macroscopic strains are localized in the film. These localized strains can be several orders of magnitude larger than the macroscopic strains in the region and have a large impact on the liquid pressure.

A HCII value larger than 1.0 does not guarantee that a hot crack will be solidified into the solid phase. For example, if the liquid pressure drop decreases, then the pore can contract and the crack may heal. Instead we consider a permanent hot crack to form when the HCII value is larger than 1.0 at the location of the terminal solidification isotherm. Assuming that all terminal liquid instantly solidifies at the terminal solidification temperature, a hot crack that is passed by this isotherm can never be healed and therefore becomes a permanent crack in the solid phase. Thus, hot cracking is considered to occur in a GBLF if the HCII value is larger than 1 at the terminal solidification location of the GBLF. A hot crack index (HCI) was then defined as the length along a GBLF where the HCII value is larger than 1.0 as follows:

$$\mathrm{HCI} = \int_{s_{ci}} ds \qquad (1)$$

where s is a coordinate along the GBLF track, that for example, can be along the columnar grain growth direction. Details can be found in [7]. The integration path s_{ci} is the part of the GBLF track where the HCII value has been larger than 1 at the intersection with the terminal solidification isotherm, see Figure 4.

If the crack propagation is small, the HCI value is assumed to be an estimation of the total crack length in the GBLF.

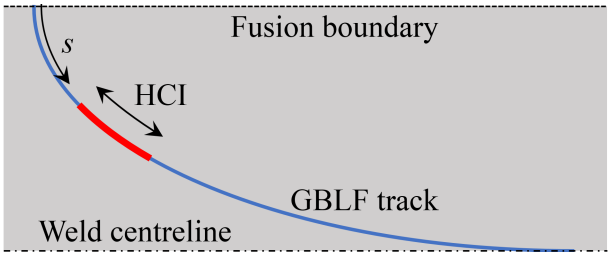

Fig. 4. Schematic representation of the HCI. The welding direction is from left to right. The shown GBLF track is located between columnar grains that extend from the fusion boundary and align with the weld centerline. The GBLF track also extends in the normal direction to the page.

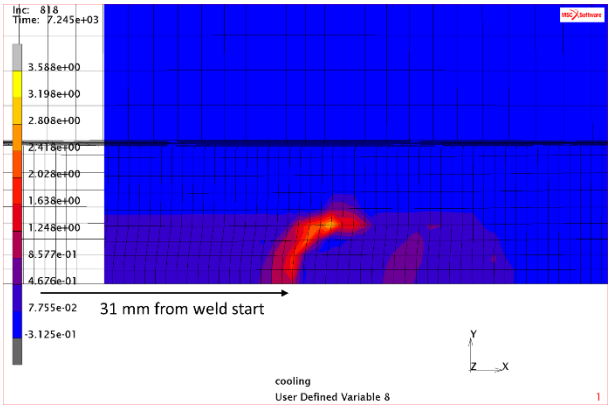

Fig. 5. Location of hot cracks predicted using the intuitive crack criterion at an augmented strain of 0.8 %.

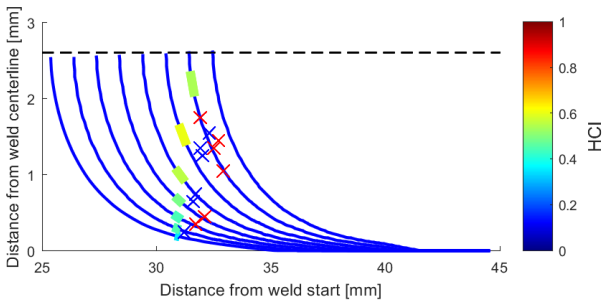

Fig. 6. HCI for Varestraint test with 0.8% augmented strain, evaluated by the physically based criterion. The blue lines correspond to GBLF traces close to the surface, separated by 1 mm at the fusion line. The welding direction is from left to right. The red crosses are crack tip locations found by stereomicroscope analysis in three Varestraint tests with 0.8% strain. The blue crosses correspond to crack tip locations in two Varestraint tests with 1.1% strain.

5 Calculated results

When the intuitive crack criterion is used, the result can conveniently be displayed directly on the finite element model in the same way as stress, strain and temperature fields are displayed. This is shown in Figure 5, which shows the value of the index in a region close to the end of the weld. The distance from the start of the weld is marked by the arrow in the figure.

When the physically based criterion is used, the HCI value is calculated after the FE analysis is completed, in a separate post processing step. The HCI value is integrated along several GBLF traces. The result is shown in Figure 6.

6 Comparison

Both the simple intuitive crack criterion and the physically based crack criterion were able to position the region where hot cracks are visible along the length of the weld. The main difference with respect to position is the position in the width direction of the weld. The intuitive crack criteria show that the largest risk for hot cracks is in or near the region of the fusion boundary of the weld, see Figure 5. The physically based crack criterion shows that hot cracks are most likely to appear about half way between the weld center line and the fusion boundary, see Figure 6. This is also the region where hot cracks appear in the experiments. Both figures show the final state after the Varestraint test has completed, as seen from above. There is a symmetry plane in the middle of the weld, at the bottom of the figures. Therefore, only half the weld is shown.

The strain needed for crack initiation is about the same for both the intuitive crack criteria and the physically based crack criteria.

7 Conclusions

From a simplicity viewpoint, the intuitive crack criterion is the best because a mesh from a traditional welding mechanics simulation is good enough, and the result is available as soon as the FE simulation is completed. The physically based crack criteria require an extra post processing step and a finer FE mesh to work as intended. This makes it more computational heavy.

When accuracy is considered, the physically based crack criterion is preferred. Not only is it better at pinpointing the region where hot cracks occur, it is also able to explain how other parameters influence the formation of hot cracks. For example, a change in welding power or speed change the development of temperature gradients and rate of solidification, both having a large effect on hot crack susceptibility. These parameters are components of the physically based criterion. It can also account for crack healing, something that the intuitive crack criteria is not capable of.

The newly developed physically based crack criterion and associated evaluation tools

are very useful for investigating the risk of hot cracking in welds of nickel-based superalloys. It is important to observe that they are not limited to just this type of alloys. It should be possible to use the same criteria to investigate the risk of hot cracks in any welded material as long as they solidify in the same manner as an alloy of metals. This is the scope for further research.

References

[1] Andersson J, Jacobsson J and Lundin C**.** *A Historical Perspective on Varestraint Testing and the Importance of Testing Parameters. In: Boellinghaus T., Lippold J., Cross C. (eds) Cracking Phenomena in Welds IV*, Springer, 2016.

[2] Lindgren L-E. *Computational Welding Mechanics.* 1 st edition, Woodhead Publishing, 2007.

[3] *Marc® 2016 Volume A: Theory and User Information. In: Marc & Mentat Docs,* MSC Software Corporation, 2016.

[4] J. Edberg, J. Andersson, Mattias Thuvander. *Evaluation of hot and warm crack problems in Ni-based alloys*, Submitted for publication.

[5] Terzi S, Salvo L, Suéry M, Limodin N, Adrien J, Maire E et al. *Scripta Materialia.* 2009;61:449

[6] Campbell J. *Complete Casting Handbook: Metal Casting Processes, Techniques and Design*. 2 nd edition, Butterworth-Heinemann, 2015.

[7] Draxler J, Edberg J, Lindgren L-E, Andersson J. *Simulation of Weld Hot Cracking in Nickel-Based Superalloys. Part I. A Pore Based Crack Criterion,* Submitted for publication.

[8] Draxler J, Edberg J, Lindgren L-E, Andersson J. *Simulation of Weld Hot Cracking in Nickel-Based Superalloys. Part II. Grain Boundary Liquid Film Pressure Model*, Submitted for publication.

Contact Author Email Address

mailto: Jonas.Edberg@ltu.se

Copyright Statement